CALCULATION AND EXPERIMENTATION OF THE COMPOUND LAYER THICKNESS IN GAS AND PLASMA NITRIDING OF IRON[*]

S. R. HOSSEINI[1], F. ASHRAFIZADEH[2**] AND A. KERMANPUR[2]

[1]Dept. of Materials Engineering, Malek-ashtar University of Technology, Isfahan 83145-115, I. R. of Iran
[2]Dept. of Materials Engineering, Isfahan University of Technology, Isfahan 8415683111, I. R. of Iran
Email: ashrafif@cc.iut.ac.ir

Abstract– Thickness of compound layers formed on the surface of pure iron during the nitriding process was analytically calculated and compared with experimental data in the gaseous and plasma nitriding. Plasma nitriding was carried out on a high purity iron substrate at a temperature of $550^{\circ}C$ in an atmosphere of 75 vol. % H_2 and 25 vol. % N_2 for various nitriding times. The thickness of compound layers was evaluated by several characterization techniques including optical microscopy, SEM and XRD. Using the Fick's first diffusion law and a mass conservation rule, two separate equations were developed for predicting the thickness of the binary compound layers; epsilon (ε) and gamma prime (γ'), in terms of the nitriding process parameters. The results of modelling indicated good agreement with the experimental data, provided that appropriate correction factors are applied. The flexibility and reliability of the models were increased by introducing two factors, K_{ε} and $K_{\gamma'}$; the calculated curves corresponded well with both gaseous and plasma nitriding experimental data.

1. INTRODUCTION

Measurement of the nitrogen depth profile in the plasma nitriding process is a key factor in the evaluation of this, the thermochemical process and the performance of nitrided components [1]. Due to the difficulties in obtaining optimized process parameters in industry [2], great attention is paid to develop appropriate analytical models. In principle, design with surface engineering involves three stages: process simulation, property simulation and service behaviour simulation. In spite of efforts made in recent years, published works on the modelling of the nitriding process are insufficient to predict, in general, the influence of dominant parameters [3].

The compound layer thickness is one of the most important factors affecting the tribological properties of the nitrided components and, during the last two decades, efforts have been made to calculate it in the gas and plasma nitriding process. Metin and Inal [4] tried to clarify the formation and growth kinetics of nitrides on the surface of pure iron during ion-nitriding and their contribution to the process mechanism. A parabolic relation was evaluated between the case depth and nitriding time. Somers and Mittemeijer studied layer growth kinetics on gaseous nitriding of pure iron and, then, evaluated diffusion coefficients for nitrogen in iron nitrides [5]. Du and Agren made a theoretical treatment of nitriding and nitrocarburizing iron [6]. They developed mathematical models for both processes based on the Fe-N and the Fe-C-N system taking into account the diffusion of nitrogen and carbon atoms through various phases. Torchane *et al* [7] tried to control the growth kinetics of iron nitride layers in the gas nitriding process

---

based on the binary Fe-N system. Dimitrov *et al* [8] modelled the formation of nitride layers during plasma nitriding of pure iron. They used the generalized Wagner diffusion model [9] to analyse the layer formation and growth in plasma nitriding experiments. The proposed model predicted the violation of the parabolic law of growth for both the compound and the diffusion zone of the plasma nitrided iron.

Maldzinski *et al* [10] made possibilities for controlling the gas nitriding process by simulation of the growth kinetics of nitride layers. Yan, Yan and Bell presented a numerical simulation for the nitrided layer growth and nitrogen distribution in ε, γ' and α-Fe during pulse plasma nitriding of pure iron at 520°C [11]. The results showed that the nitrided layer consists of *ε, γ′* and *α*-Fe phases, and its thickness growth followed a parabolic law. Belmonte *et al* [12] provided a numerical model for nitrogen diffusion in pure iron accounting for the concentration dependence of the intrinsic diffusivity of nitrogen. Comparison of the results of their work with the experimental data available in the literature revealed a number of discrepancies. In spite of this, the thickness of the layers versus the square root of the nitriding time at a temperature of 843 K was calculated.

Keddam *et al* carried out several works on the modelling of the nitriding process for pure iron [13-16]. Emphasis was made on the choice of the nitriding potential of the $NH_3–H_2$ atmosphere on the microstructural constitution and growth kinetics of the nitrided layers [13]. They applied a diffusion model based on the Fick's laws in order to study the growth kinetics of the ε and γ′ phases during gas nitriding of pure iron [14]. Keddam *et al* also designed a simplified diffusion model to predict the thickness of the nitrided layer and the nitrogen profile in pure iron [15]. Furthermore, they modelled the pulse plasma nitriding process of pure iron using a kinetic model derived from the Fick's laws [16].

Most of the previous works emphasized the modelling of the gas nitriding process. A few works concentrated on modeling the compound layer growth during the plasma nitriding process.

Recently, the authors developed analytical solutions to predict the distribution of nitrogen concentration [17] and compound layer growth [18] during nitriding of pure iron. An analytical approach model based on experimental data was used to evaluate the accurate depth profile of the diffusion zone in the plasma nitrided iron [19]. In the present paper, the models for compound layers calculation have been modified by introducing correlation factors to increase their flexibility and reliability. The analytical treatment for the calculation of the compound layer thickness is based on the Fick's first diffusion law, mass conservation rule and the thermodynamic description of the Fe-N phase diagram. Plasma nitriding experiments were carried out and the compound layer thickness was measured for the validation of the models. Moreover, gas nitriding experimental data were obtained from literature to validate the models.

2. ANALYTICAL PROCEDURE

a) Formation of compound layers

The solubility of nitrogen in iron at room temperature is very limited and reaches a maximum of 0.4 at% (0.1 wt %) at 592°C. In the nitriding process of iron, when the nitrogen concentration exceeds the solubility limit, extra nitrogen atoms make stoichiometric compounds with iron atoms, therefore, precipitating intermediate iron nitrides. The surface composition of the nitrided iron can be predicted by considering the Fe-N binary phase diagram. Based on this diagram [20], several phases and compounds including alpha (α), gamma (γ), gamma prime (γ′), epsilon (ε), zeta (ξ), *etc* may theoretically be formed during the nitriding process.

As the nitrogen potential on the surface of the components does not commonly exceed 10wt%, some of the phases present in the equilibrium diagram, for example ξ and nitrogen rich compounds, cannot be formed during the nitriding process. Therefore, the surface structure of the nitrided iron generally includes α-Fe(N) diffusion zone (solid solution of nitrogen in α-Fe), γ′ and ε compound layers. The γ′ nitride phase

is an intermediate compound with a stoichiometry close to Fe_4N with 20 at% (5.9 wt %) nitrogen. The ε nitride is an intermediate phase that is formed in a range of nitrogen concentration, thus, it is generally demonstrated as $Fe_{2-3}N$. Theoretically, the maximum solubility of nitrogen in the ε phase is about 33at% (11wt %), but according to the nitrogen activity in the actual nitriding process, the nitrogen concentration in the ε nitride phase does not generally exceed 9 wt%. The nitrogen concentration in ε and γ' layers as well as α diffusion zone are schematically demonstrated in Fig. 1.
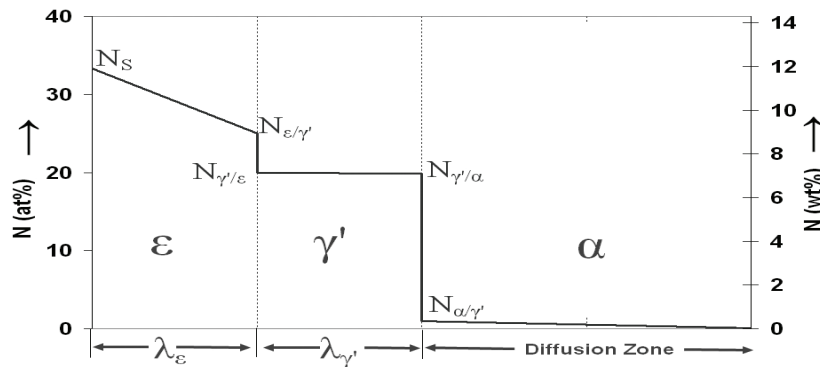

Fig. 1. Prediction of nitrogen distribution in layers that can be formed on the surface of nitrided iron

b) Solution of the governing equations

General form of the Fick's first law for the nitriding process can be expressed as:

$$J_i = -D_i \frac{\partial N_i(x,t)}{\partial x} \qquad i = \varepsilon, \gamma', \alpha \text{ phase} \qquad (1)$$

Rewriting the Fick's first law for nitrogen diffusion in each phase yields the following expressions:

$$J_\varepsilon = -D_\varepsilon \times (\partial N_\varepsilon / \partial x) \qquad (2)$$

$$J_{\gamma'} = -D_{\gamma'} \times (\partial N_{\gamma'} / \partial x) \qquad (3)$$

$$J_\alpha = -D_\alpha \times (\partial N_\alpha / \partial x) \qquad (4)$$

Where, J_ε, $J_{\gamma'}$ and J_α are nitrogen fluxes, D_ε, $D_{\gamma'}$ and D_α are the diffusion coefficients of nitrogen, and N_ε, $N_{\gamma'}$ and N_α are nitrogen concentrations in the ε, γ' and α phases, respectively.

The mass conservation rule for the compound layers can be used in common with other investigations [13, 14]. Considering Fig. 1, for the above mentioned case, the mass conservation rule at the interfaces between layers can be expressed as:

$$W_\varepsilon \frac{d\lambda_\varepsilon}{dt} = [J_\varepsilon - J_{\gamma'}]_{X = \lambda_\varepsilon} \qquad (5)$$

$$W_{\gamma'} \frac{d(\lambda_\varepsilon + \lambda_{\gamma'})}{dt} = W_{\gamma'} \frac{d\lambda_{\gamma'}}{dt} + W_{\gamma'} \frac{d\lambda_\varepsilon}{dt} = [J_{\gamma'} - J_\alpha]_{X = \lambda_\varepsilon + \lambda_{\gamma'}} \qquad (6)$$

Where λ_ε and $\lambda_{\gamma'}$ are the thickness of ε and γ' layers, respectively. W_ε and $W_{\gamma'}$ are defined as follows:

$$W_\varepsilon = N_{\varepsilon/\gamma'} - N_{\gamma'/\varepsilon} \qquad (7)$$

$$W_{\gamma'} = N_{\gamma'/\alpha} - N_{\alpha/\gamma'} \qquad (8)$$

$N_{\varepsilon/\gamma'}$, $N_{\gamma'/\varepsilon}$, $N_{\gamma'/\alpha}$ and $N_{\alpha/\gamma'}$ are the concentration of nitrogen atoms at interfaces of the layers as demonstrated in Fig. 1.

With the assumption of equilibrium in the Fe-N system, the initial and boundary conditions can be expressed as:

    I. Maximum concentration of nitrogen in ε-Fe$_{2-3}$N nitride reaches 11.14 wt%, when it is assumed as Fe$_2$N with a nitrogen content of 33.33at%. The concentration of nitrogen in ε-Fe$_{2-3}$N nitride decreases to a minimum value of 7.71 wt% near the γ' interface, when it is assumed as Fe$_3$N including 25.0 at%N.

   II. Concentration of nitrogen in γ' nitride is approximately equal to 5.9wt%, assuming to be the stoichiometric compound of Fe$_4$N with 20at%N. According to the data from the literature [13], it is in the range of 5.76 to 5.90wt%.

  III. Maximum solubility of nitrogen in α-iron, at 590°C (863K) and at the equilibrium with γ' nitride, can be considered approximately 0.1wt% (0.4at %). The nitrogen concentration approaches zero at a certain depth into the substrate, far from the α/γ' interface.

Considering boundary conditions I and II, and referring to Fig. 1, the nitrogen concentration at interfaces between the ε, γ' and α layers can be expressed as:

$$N_{\varepsilon/\gamma'} \approx 7.71\,\text{wt}\% \tag{9}$$

$$N_{\gamma'/\varepsilon} \approx 5.91\,\text{wt}\% \tag{10}$$

$$N_{\gamma'/\alpha} \approx 5.76\,\text{wt}\% \tag{11}$$

The nitrogen concentration in the boundary of the α diffusion phase at equilibrium with the γ' nitride can be written as [15, 21]:

$$N_{\alpha/\gamma'} = 12.3\exp(\frac{-4176}{T}).......[\text{wt}\%] \tag{12}$$

On the other hand, the growth of compound layers follows a parabolic law, and can be expressed as:

$$\lambda_i = b_i\sqrt{t} \tag{13}$$

Where λ_i, b_i and t are the thickness of i layer, the constant of the growth rate and the nitriding time, respectively. Therefore, at a constant temperature for ε and γ' layers:

$$\lambda_\varepsilon = b_\varepsilon\sqrt{t} \tag{14}$$

$$\lambda_{\gamma'} = b_{\gamma'}\sqrt{t} \tag{15}$$

Where b_ε and $b_{\gamma'}$ are constants of the growth rate. Derivation of the above equations gives:

$$\frac{d\lambda_\varepsilon}{dt} = \frac{b_\varepsilon}{2\sqrt{t}} \tag{16}$$

$$\frac{d\lambda_{\gamma'}}{dt} = \frac{b_{\gamma'}}{2\sqrt{t}} \tag{17}$$

c) Calculation of ε nitride thickness

Taking into account the Eqs. (7), (9), (10) and (16), Eq. (5) can be rearranged as:

$$\frac{0.9b_\varepsilon}{\sqrt{t}} = [J_\varepsilon - J_{\gamma'}]_{X = \lambda_\varepsilon} \tag{18}$$

The nitrogen concentration distribution in ε, calculated in the previous work [17] and developed here,

$$N_\varepsilon = N_s + \frac{7.712 - N_s}{\mathrm{erf}(\frac{\lambda_\varepsilon}{2\sqrt{D_\varepsilon t}})} \, \mathrm{erf}\left(\frac{x}{2\sqrt{D_\varepsilon t}}\right) \tag{19}$$

Where N_s is the nitrogen concentration at the surface of the work piece as demonstrated in Fig. 1. Derivation and simplification of the above equation yields nitrogen flux at the interface between the ε and γ' nitride as:

$$J_\varepsilon\Big|_{x = \lambda_\varepsilon} \approx 3.4 \frac{D_\varepsilon}{\lambda_\varepsilon} \tag{20}$$

On the other hand, nitrogen concentration distribution in γ', calculated in a previous work [17] and developed here, is recommended as:

$$N_{\gamma'} = \frac{0.14\lambda_\varepsilon + 5.90\lambda_{\gamma'}}{\lambda_{\gamma'}} - \frac{0.28\sqrt{D_{\gamma'}t}}{\lambda_{\gamma'}} \, \mathrm{erf}\left(\frac{x}{2\sqrt{D_{\gamma'}t}}\right) \tag{21}$$

Derivation and simplification of the above equation yields nitrogen flux at the interface between the γ' layer and α zone as;

$$J_{\gamma'} = 0.14 \frac{D_{\gamma'}}{\lambda_{\gamma'}} \tag{22}$$

Replacing Eqs. (20) and (22) in Eq. (18) and considering Eq. (14), the constant of the ε nitride growth rate, b_ε, and thus the thickness of the ε layer can be calculated versus time and diffusion coefficients as:

$$b_\varepsilon \approx \sqrt{4D_\varepsilon - 0.2D_{\gamma'}} \tag{23}$$

$$\lambda_\varepsilon \approx \sqrt{(4D_\varepsilon - 0.2D_{\gamma'}).t} \tag{24}$$

d) Calculation of γ' nitride thickness

For the calculation of γ' nitride thickness, Eqs. (7), (8), (16) and (17) are replaced in Eq. (6). Function $12.3\exp(-4176/T)$ indicates the solubility limit curve at α phase. Maximum solubility of nitrogen in α phase ($N_{\alpha/\gamma'}$) can reach 0.1wt% at a temperature of 592°C. Thus, Eq. (6) will be changed to:

$$2.83(\frac{b_\varepsilon}{\sqrt{t}} + \frac{b_{\gamma'}}{\sqrt{t}}) = \left[J_{\gamma'} - J_\alpha\right]_{x = \lambda_\varepsilon + \lambda_{\gamma'}} \tag{25}$$

The constant of the ε nitride growth rate, b_ε, calculated previously, is summarized in Eq. (23).

Similar to the previous section, $J_{\gamma'}$ can be replaced from Eq. (22). Equation (4) can be used for the calculation of J_α. The nitrogen concentration distribution in α is calculated by the authors [17] and expressed as:

$$N_\alpha = 12.3\exp(\frac{-4175.9}{T})\left(1 - \mathrm{erf}(\frac{x}{2\sqrt{D_\alpha t}})\right) \tag{26}$$

Derivation of this equation yields:

$$\frac{\partial N_\alpha}{\partial x} = \left(\frac{-12.3}{2\sqrt{D_\alpha t}}\right).\exp\left(\frac{-4176}{T}\right) \bigg/ \left(1 - \mathrm{erf}(\frac{\lambda_\varepsilon + \lambda_{\gamma'}}{2\sqrt{D_\alpha t}})\right) \tag{27}$$

The amount of factor $12.3\exp(-4176/T)$ at the maximum nitriding temperature, *e.g.* 592°C, will be about 0.1 wt%. Considering the above equation, Eq. (4) and simplification yield:

$$J_\alpha \approx \frac{0.1 D_\alpha}{2\sqrt{D_\alpha t}} \tag{28}$$

Replacing Eqs. (22) and (28) in Eq. (25) with further simplification, the constant of the γ' nitride growth rate, $b_{\gamma'}$, and thus $\lambda_{\gamma'}$ can be calculated versus time and diffusion coefficient;

$$b_{\gamma'} \approx 0.5\left[-(b_\varepsilon + 0.02\sqrt{D_\alpha}) + \sqrt{(b_\varepsilon + 0.02\sqrt{D_\alpha})^2 + 0.2D_{\gamma'}}\right] \tag{29}$$

$$\lambda_{\gamma'} \approx 0.5\left[-(b_\varepsilon + 0.02\sqrt{D_\alpha}) + \sqrt{(b_\varepsilon + 0.02\sqrt{D_\alpha})^2 + 0.2D_{\gamma'}}\right].\sqrt{t} \tag{30}$$

3. EXPERIMENTAL PROCEDURE

a) Substrate and treatments

Pure iron, a popular material for nitriding studies, was used as substrate material in common with other investigations [5-7]. In this work, disc-shaped ARMCO iron samples with a 25 mm diameter and 5 mm thickness were prepared from 30 mm diameter bars. Table 1 shows the chemical composition and impurity levels of the substrate material. The specimens were ground, cleaned in acetone and dried before plasma nitriding. Plasma nitriding was carried out in a semi-industrial unit with a 5kW DC power supply. The general sequence of the plasma nitriding experiments started with sputter cleaning and heating the specimens to 550 °C (823 K) ±5 °C in an atmosphere composed of 50 vol.% H_2 and 50 vol.% Ar. Sputter cleaning took place in 0.01 Torr pressure of H_2-Ar mixture for approximately 10 min, after which the heating cycle was started. Upon reaching the prescribed temperature, the atmosphere was switched to a mixture of 75 vol. % H_2 and 25 vol. % N_2 and the nitriding cycle began. Total gas pressure was about 5 Torr in all tests and the selected times were 1, 2, 5 and 10 hours. After the nitriding cycle was completed, the power supply was switched off and the samples were allowed to cool down in the furnace under vacuum to obtain a moderate cooling condition. Samples were collected from the chamber at room temperature.

Table 1. Chemical composition and impurities of ARMCO iron substrate material (wt %)

C	Si	Mn	Cr	Mo	Al	V	Ni	Cu	Ti	P	S	Fe
<0.0050	<0.0050	<0.050	<0.0100	<0.0080	<0.0080	0.0270	<0.030	0.0215	<0.0060	<0.0080	0.0090	99.81

b) Surface characterization

Metallographic examinations were performed on cross sections of the samples, prepared by a standard grinding and polishing procedure. After plasma nitriding, typical samples were sectioned, nickel electroplated in Watts plating bath, mounted in bakelite, ground, polished (0.3 μm Al_2O_3), and etched in 2% Nital solution (2% HNO_3–98% CH_3CH_2OH). Microstructural observations were carried out using

an optical microscope and SEM (Philips XL 30). A thin layer of gold was sputtered on the surface of samples for increasing electron conduction in the SEM chamber.

XRD analyses were performed by a PHILIPS X'Pert diffractometer. Cu Kα radiation, the wavelength Kα$_1$ of 1.54056 Å and Kα$_2$ of 1.54439 Å with an intensity ratio (Kα$_2$/ Kα$_1$) of 0.5 was employed. The X-ray generator was operated at 40 kV and 30 mA. The patterns were obtained with a 2θ step size of 0.04°, in the range of 20–140°, with a time constant of one second.

4. RESULTS AND DISCUSSION

Equation (24) indicates the growth of the ε layer versus two dominant parameters, time and the diffusion coefficient. Equation (30) indicates the growth and movement of the γ' layer adjacent to the ε towards the substrate, as a function of time and diffusion coefficient. Growth of the ε layer, Eq. (24), depends on the diffusion coefficient of nitrogen in both the ε and γ' layers, while growth of the γ' layer, Eq. (30), depends on the diffusion coefficient of nitrogen in three phases of ε, γ', and α. This means that the characteristics of each layer can affect the growth of other layers; for example, diffusion of nitrogen through the ε layer (input to the γ') as well as diffusion of nitrogen through α zone (output of the γ') could both affect the growth rate of the γ' layer. Thus, the diffusion coefficient of nitrogen in the ε nitride and α zone, D_ε and D_α, must also be taken into account. In the proposed equations, all affecting diffusion coefficients are considered for evaluation of the layer thickness.

Diffusion coefficient of nitrogen in the ε, γ' and α phase as a function of temperature was determined elsewhere as [17, 21]:

$$D_\varepsilon = 2.1 \times 10^{-8} \exp\left(\frac{-93517\,\frac{J}{mol}}{RT}\right), \quad [m^2/s] \qquad (31)$$

$$D_{\gamma'} = 1.7 \times 10^{-9} \exp\left(\frac{-64000\,\frac{J}{mol}}{RT}\right), \quad [m^2/s] \qquad (32)$$

$$D_\alpha = 6.6 \times 10^{-7} \exp\left(\frac{-77900\,\frac{J}{mol}}{RT}\right), \quad [m^2/s] \qquad (33)$$

The values of the diffusion coefficient of nitrogen in ε and γ' nitride as well as α zone, calculated at different temperatures by means of Eqs. (31), (32) and (33), respectively, are indicated in Table 2. Increasing the nitriding temperature from 500 to 580°C results in increasing the diffusion coefficient of nitrogen in all phases at almost the same rate. At any given temperature, the diffusion coefficient of nitrogen in the α phase is about 100 and 10 times more than that of ε and γ' nitride, respectively. Increasing the nitriding temperature from 500 to 580°C leads to a decrease in the ratios of D_α/D_ε and $D_{\gamma'}/D_\varepsilon$, while it increases the ratio $D_\alpha/D_{\gamma'}$.

Combining Eqs. (31) and (32) with Eq. (24) yields a complicated equation indicating the growth of the ε layer versus two important parameters of the nitriding process; temperature and time. Similarly, by

combining Eqs. (30), (31), (32) and (33), the thickness of the γ' layer can be evaluated versus temperature and time.

Table 2. Diffusion coefficient of nitrogen in ε, γ' and α at different temperatures

Nitriding Temperature	°C	500	510	520	530	540	550	560	570	580
	K	773	783	793	803	813	823	833	843	853
Diffusion Coefficient of Nitrogen [$10^{-14} m^2/s$]	ε	1.0	1.2	1.5	1.7	2.1	2.4	2.9	3.4	3.9
	γ'	7.9	9.0	10.2	11.5	12.9	14.5	16.3	18.1	20.2
	α	359.4	419.6	487.9	565.3	652.5	750.6	860.5	983.3	1120.2

Considering the above equations, it can be understood that the growth rate of each layer is high at the primary stages of the nitriding process, but it decreases rapidly after about two hours. This phenomenon can be explained by considering the parabolic growth rate. The growth rates of both the ε and γ' layers increase rapidly with increasing the nitriding temperature, as related to the diffusion coefficient of nitrogen.

In addition to the effect of nitriding temperature and time on the growth rate, and thereby the thickness of the layers, there are several parameters affecting the kinetics of the layers growth. The important parameters are the type of nitriding process, *i.e.*, gas or plasma nitriding, surface concentration, and the composition dependence of the nitrogen diffusivities in the iron nitride phases. Due to the number and versatile nature of such parameters, it is difficult to yield a model that can include all the important factors on the kinetics and thus the thickness of compound layers. If an ideal condition based on the binary Fe-N system is established leading to a surface concentration of nitrogen necessary for the complete formation of Fe_3N, *i.e.*, 11.15 wt%, Eqs. (24) and (30) may predict the growth of ε and γ' layers, respectively. If the condition changed from ideal, *e.g.* the surface concentration decreased below 11.15 wt% as normally happens under actual nitriding processes, the latter models cannot be expected to indicate the growth of compound layers.

In order to develop a model that takes into account the actual parameters of nitriding processes, in the present work Eqs. (24) and (30) are re-evaluated respectively as;

$$\delta_\varepsilon = K_\varepsilon b_\varepsilon \sqrt{t} = K_\varepsilon \sqrt{(4D_\varepsilon - 0.2D_{\gamma'})t} \tag{34}$$

$$\delta_{\gamma'} = K_{\gamma'} \left[\sqrt{(b_\varepsilon + 0.02\sqrt{D_\alpha})^2 + 0.2D_{\gamma'}} - (b_\varepsilon + 0.02\sqrt{D_\alpha}) \right] \sqrt{t} \tag{35}$$

where δ_ε and $\delta_{\gamma'}$ are corrected thickness of ε and γ' nitride layers, K_ε and $K_{\gamma'}$ are the correlation factors depending on the process parameters rather than nitriding temperature and time. Under ideal conditions, these factors have a value of 1.0 and 0.5 respectively. Far from ideal conditions, K_ε and $K_{\gamma'}$ will be changed, *e.g.* decreasing the surface concentration, K_ε approaches zero.

Figure 2 shows the thickness of ε nitride versus K_ε and the nitriding time at constant nitriding temperature, 550°C. Thickness of γ' nitride versus $K_{\gamma'}$ and nitriding time at constant nitriding temperature, 550°C, are presented in Fig. 3. It can be concluded that, at any given K, the growth rate of each layer is high at the primary stages of the nitriding process, but it decreases rapidly after about 1-3 hours. This phenomenon can be explained by considering the parabolic growth rate. Moreover, the thickness of both ε and γ' layers increases rapidly with increasing K_ε and $K_{\gamma'}$, respectively.
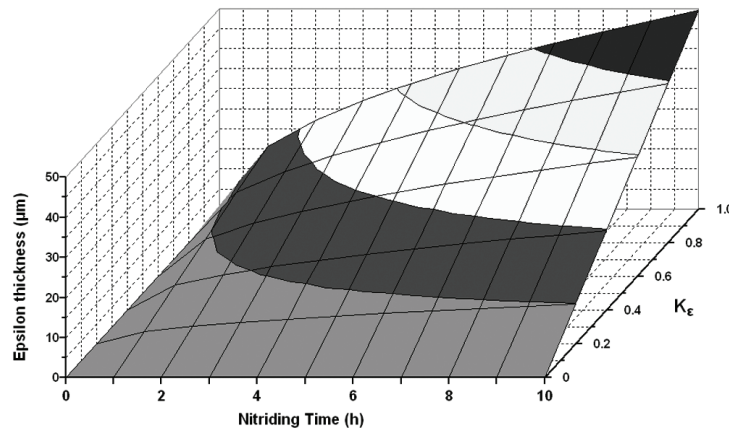
Fig. 2. Thickness of epsilon nitride versus K_ε and nitriding time at constant nitriding temperature, 550°C, in three dimensional scales
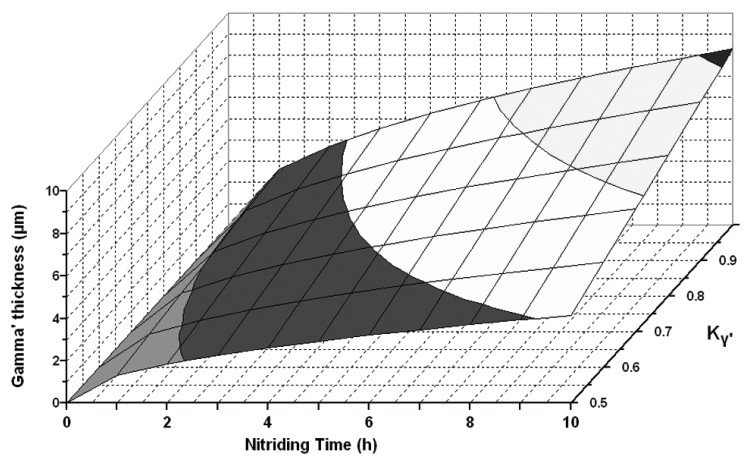

Fig. 3. Thickness of gamma prime nitride versus $K_{\gamma'}$ and nitriding time at constant nitriding temperature, 550°C, in three dimensional scales

For evaluation of the reliability of the above models, the thickness of ε and γ' layers at several given K_ε and $K_{\gamma'}$ were calculated and compared with the experimental data of the present work along with data obtained from the literature [5-7 and 10]. Figure 4 shows the calculated thickness of ε and γ' layers versus nitriding time at 570°C with K_ε=0.3 and $K_{\gamma'}$=0.6, respectively, and compared with data reported by Somers and Mittemeijer in the gas nitriding process [5]. They used a gas mixture of NH_3-H_2 with 56.1 vol% NH_3 (r_N=6.06x10^{-3} Pa^{-1}) and good agreement is observed between their experimental data and the purposed model.
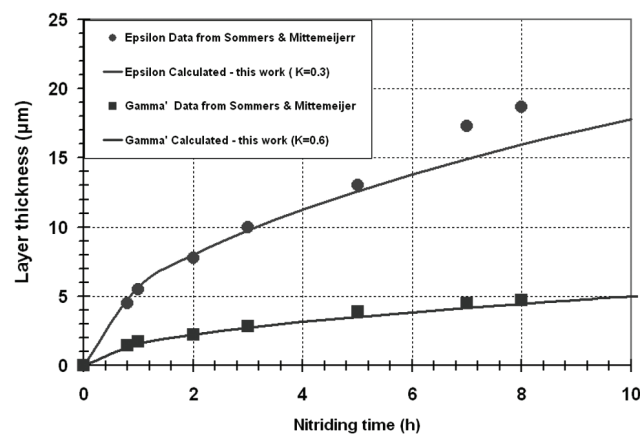

Fig. 4. Thickness of ε and γ' layers versus nitriding time at 570°C calculated in this work, compared with data from Somers and Mittemeijer [5]

Thickness of ε and γ' layers at a temperature of 575°C were calculated at $K_\varepsilon=0.2$ and $K_{\gamma'}=0.5$, respectively, and compared with data reported by Du and Agren [6] as demonstrated in Fig. 5. Their experimental findings in the gas nitriding process with nitrogen surface content of 8 wt%, evidenced that the results of the present modelling correspond very well with these data.
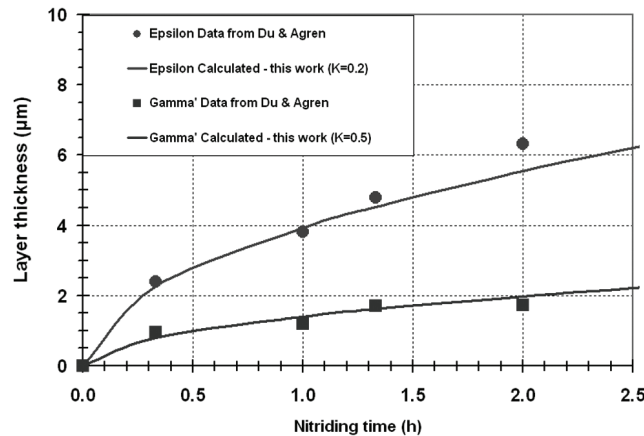

Fig. 5. Thickness of ε and γ' layers at 575°C calculated in this work,
compared with data from Du and Agren [6]

Figure 6 shows the thickness of ε and γ' layers versus nitriding time at a temperature of 570°C calculated with $K_\varepsilon=0.2$ and $K_{\gamma'}=1.7$, respectively, and compared with data published by Torchane, et al [7]. Their experiments were performed under the condition of gas nitriding in a mixture of NH_3-N_2-H_2 with a nitrogen surface content of 8.5 wt%. It is clear that the results of the current model correspond very well with the experimental data.
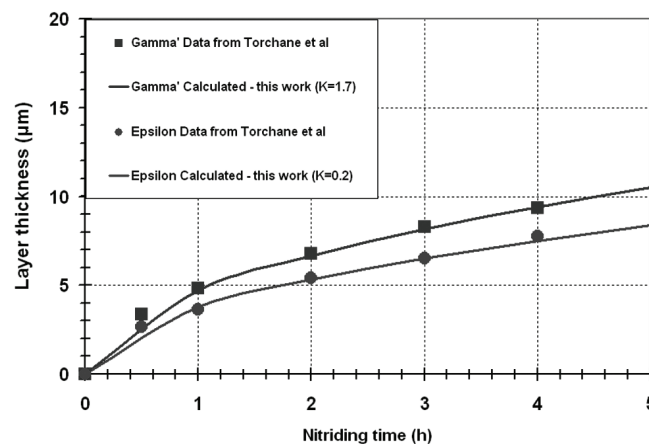

Fig. 6. Thickness of ε and γ' layers versus nitriding time at 570°C calculated in
this work, compared with data from Torchane *et al* [7]

Thickness of ε and γ' layers versus nitriding time at a temperature of 550°C were calculated at $K_\varepsilon=0.25$ and $K_{\gamma'}=0.5$, respectively, and compared with data reported by Maldzinski and co-workers [10], as demonstrated in Fig. 7. These measurements were performed in the gas nitriding process with a nitrogen surface content of 9.15 wt% and good agreement is observed between the results of the present modelling and their experimental data.

Figure 8 illustrates a typical SEM micrograph of the cross section of the plasma nitrided iron in the present work. It can be seen that, the compound layer is composed of two separated layers; thickness of the outer layer, epsilon, is much lower than that of the inner one, gamma prime.
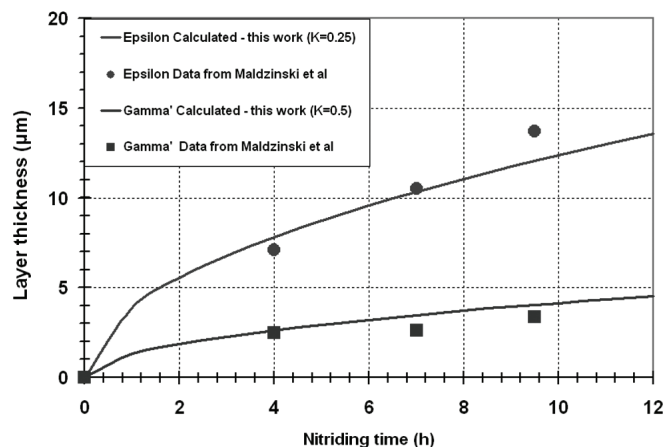
Fig. 7. Thickness of ε and γ' layers versus nitriding time at 550°C calculated in this
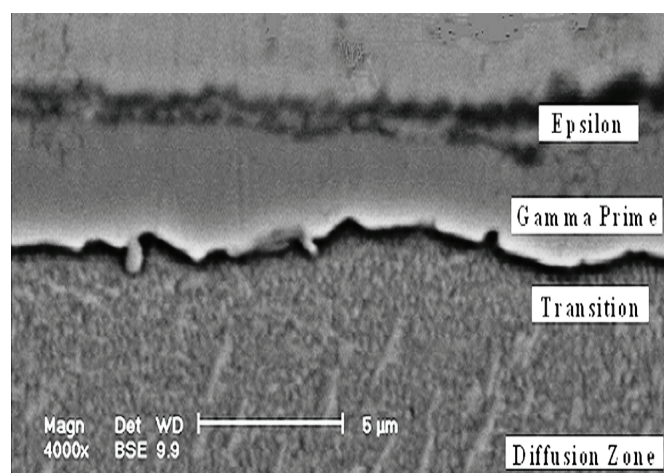work compared with data from Maldzinski *et al* [10]

Fig. 8. SEM micrograph of the cross section of the plasma nitrided iron at 550°C

Figure 9 shows an XRD pattern of two plasma nitrided samples compared with that of untreated pure iron. For the untreated sample, there are five peaks diffracted from (110), (200), (211), (220) and (310) planes of pure iron. After one hour plasma nitriding, several peaks from epsilon and gamma prime nitrides appeared on the pattern. This means that one hour plasma nitriding is sufficient to begin the continuous formation of both epsilon and gamma prime nitrides. In other words, nucleation was completed, incubation time was finished and continuous layer growth was started after one hour nitriding. According to an investigation made by Sun and Bell [22], there is a threshold nitrogen potential at which the compound layer, epsilon or gamma prime nitrides, can be nucleated. For plasma nitriding of pure iron at a temperature of 560°C, in an atmosphere containing at least 6 vol.%N_2, almost one hour is sufficient for the nucleation of the compound layer. If nitrogen potential exceeds this limit, the incubation time for nucleation and growth of the compound layer decreases rapidly. In the present research, plasma nitriding was performed at a temperature of 550°C, almost similar to the work done by Sun and Bell. The nitriding potential used in this investigation was 25 vol.%N_2, which is quite more than that used for calculation by the above mentioned researchers. At this nitriding potential, the compound layer can nucleate and grow at the primary stage of nitriding. Extrapolating of the curves reported by Sun and Bell implies that if nitrogen percentage exceeds 15 vol.%, nitrides can nucleate and grow at quarter of an hour.

Figure 10 shows the thickness of the ε and γ' layers versus nitriding time at 550°C calculated with K_ε=0.05 and K_γ=0.7, respectively, and compared with experimental data obtained in the present work. It is observed that the results of the present modelling correspond well not only with the experimental data

under gas nitriding reported by other researchers, but also with experimental data under the plasma nitriding measured in this work.
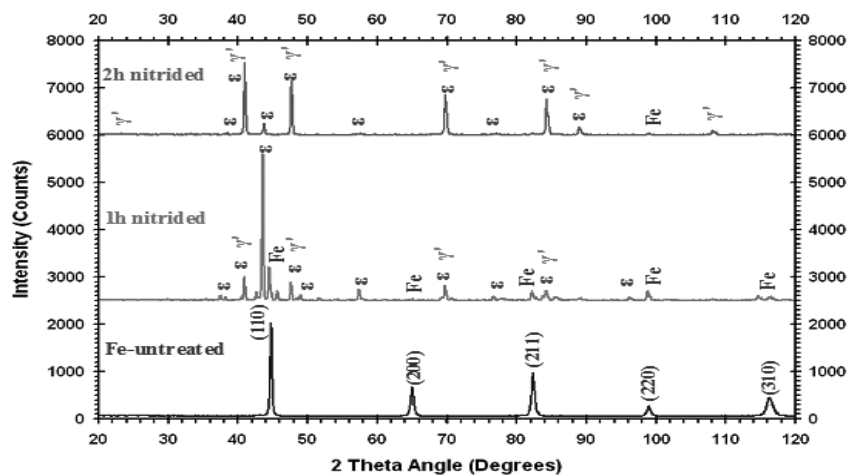

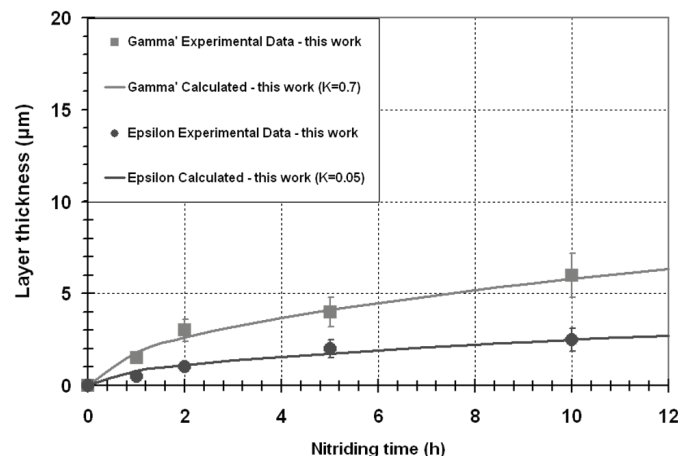Fig. 9. XRD pattern of two plasma nitrided samples compared with that of untreated pure iron

Fig. 10. Thickness of ε and γ' layers versus nitriding time at 550°C calculated in this work
compared with plasma nitrided experimental data made in the present work

One should note that sometimes it is difficult to distinguish the ε layer from the γ' layer by metallographic examination. For example, the experimental measurements of the compound layer thickness for plasma nitriding of pure iron carried out by the authors at a temperature of 550°C showed that although there is a good agreement between the measurement and the calculated data, some minor differences still exist due to the mixing and combination of ε and γ' nitrides in plasma nitriding. On the other hand, the ε and γ' nitrides can be clearly distinguished as separated and continuous layers under the gas nitriding process. Moreover, normally ε thickness is higher than γ' nitride in gas nitriding, while under plasma nitriding condition the γ' thickness is higher than that of ε nitride. These phenomena are caused by several process parameters such as sputtering, surface reactions and bombardment of the surface by charged specious during plasma nitriding.

The correlation factors, K_{ε} and $K_{\gamma'}$, introduced in this work, increased the flexibility and reliability of the models, therefore, the calculated data corresponded very well with the experimental data in several gas and plasma nitriding conditions. In practical nitriding conditions, it would be possible to find K_{ε} and $K_{\gamma'}$ by carrying out a few experiments and then, predict the thickness of the compound layers under any nitriding cycle.

5. CONCLUSION

Based on the analytical calculation, experimental data and evidence presented in this work, the main conclusions are summarised below.

- Two analytical equations were derived for the thickness calculation of ε and γ' layers, respectively, in terms of nitriding parameters:

$$\delta_\varepsilon = K_\varepsilon . b_\varepsilon . \sqrt{t} = K_\varepsilon . \sqrt{(4D_\varepsilon - 0.2D_{\gamma'}).t}$$

$$\delta_{\gamma'} = K_{\gamma'} . \left[\sqrt{(b_\varepsilon + 0.02\sqrt{D_\alpha})^2 + 0.2D_{\gamma'}} - (b_\varepsilon + 0.02\sqrt{D_\alpha}) \right] . \sqrt{t}$$

- The equations presented in this work can be used for calculation of the compound layer thickness in various nitriding processes. The modelling results agreed very well with the experimental data under gaseous and plasma nitriding processes.
- At any given temperature, the growth rate of each layer was high at primary stages of the nitriding process, but it decreased rapidly with increasing nitriding time.
- The growth rate of both ε and γ' layers increased rapidly with increasing the nitriding temperature.
- The ε thickness is higher than the γ' nitride under gas nitriding condition, normally, while in plasma nitriding the γ' thickness is higher than that of the ε nitride.
- Correlation factors, K_ε and $K_{\gamma'}$, introduced in this work, increased the flexibility and reliability of the models; under any nitriding condition, it is possible to find the values of K_ε and $K_{\gamma'}$ by a few experimental tests. The equations are then applicable to various nitriding treatments and can be used as a practical tool to estimate the compound layer thickness of ε and γ'.

REFERENCES

1. Hosseini, S. R. & Ashrafizadeh, F. (2009). Accurate measurement and evaluation of the nitrogen depth profile in plasma nitrided iron. *Vacuum,* Vol. 83 pp. 1174-1178.
2. Aghababa, J., Ashrafizadeh, F., Azari, H. N. (2002). Effect of manufacturing parameters on the formability of low-C sheet steel. *Iranian Journal of Science and Technology, Transaction B: Engineering*, Vol. 26, No. B1, pp. 11-19.
3. Hosseini, S. R. & Ashrafizadeh, F. (2006). Application of mathematical modelling and computer simulation in heat treatment and surface engineering. *Proc. 7th Conf. Heat Treatment and Surface Engineering*, *Iranian Society of Surf. Sci. & Tech*., Isfahan, pp. 1591-1601.
4. Metin, E. & Inal, O. T. (1987). Formation and growth of iron nitrides during ion-nitriding. *Journal of Materials Science*, Vol. 22, pp. 2783-2788.
5. Somers, M. A. J. & Mittemeijer, E. J. (1995). Layer growth kinetics on gaseous nitriding of pure iron: Evaluation of diffusion coefficients for nitrogen in iron nitrides. *Metallurgical and Materials Transactions A*, Vol. 28, pp. 57-74.
6. Du, H. & Agren, J. (1996). Theoretical treatment of nitriding and nitrocarburizing of iron. *Metallurgical and Materials Transactions A*, Vol. 27, pp. 1073-1080.

7. Torchane, L., Bilger, P., Dulcy, J. & Guntois, M. (1996). Control of iron nitride layers growth kinetics in the binary Fe-N system. *Metallurgical and Materials Transactions A*, Vol. 27, pp. 1823-1835.

8. Dimitrov, V. I., D'Haen, J., Knuyt, G., Quaeyhaegens, C. & Stals, L. M. (1999). Modeling of nitride layer formation during plasma nitriding of iron. *Comp. Mat. Sci.*, Vol. 15, pp. 22-34.

9. Dimitrov, V. I., Knuyt, G., Stals, L. M., D'Haen, J. & Quaeyhaegens, C. (1998). Generalized Wagner's diffusion model of surface modification of materials by plasma diffusion treatment. *Appl. Phys. A*, Vol. 67, pp. 183–192.

10. Maldzinski, L., Liliental, W., Tymowski, G. & Tacikowski, J. (1999). New possibilities for controlling gas nitriding process by simulation of growth kinetics of nitride layers. *Surface Engineering*, Vol. 15, pp. 377-384.

11. Yan, M., Yan, J. & Bell, T. (2000). Numerical simulation of nitrided layer growth and nitrogen distribution in ε-ε-Fe_{2-3}N, γ'-Fe_4N and α-Fe during pulse plasma nitriding of pure iron. *Modelling Simul. Mater. Sci. Eng.*, Vol. 8, pp. 491-496.

12. Belmonte, T., Goune, M. & Michel, H. (2001). Numerical modeling of interstitial diffusion in binary systems, application to iron nitriding. *Mat. Sci. and Eng. A*, Vol. 302, pp. 246–257.

13. Keddam, M., Djeghlal, M. E., Barrallier, L. & Salhi, E. (2004). Computer simulation of nitrided layers growth for pure iron. *Comp. Mat. Sci.*, Vol. 29, pp. 43–48.

14. Keddam, M., Djeghlal, M. E. & Barrallier, L. (2004). A diffusion model for simulation of bilayer growth (ε/γ') of nitrided pure iron. *Mat. Sci. and Eng. A*, Vol. 378, pp. 475–478.

15. Keddam, M., Djeghlal, M. E. & Barrallier, L. (2005). A simple diffusion model for the growth kinetics of γ' iron nitride on the pure iron substrate. *Appl. Surf. Sci.*, Vol. 242, pp. 369-374.

16. Keddam, M. (2007). Surface modification of the pure iron by the pulse plasma nitriding: Application of a kinetic model, *Mat. Sci. and Eng. A*, Vol. 462, pp. 169-173.

17. Hosseini, S.R., Kermanpur, A. & Ashrafizadeh, F. (2007). Mathematical modelling of nitrogen depth profile in the nitriding of pure iron, *Proc. 8th Conference Surface Engineering and Heat Treatment, Iranian Society of Surf. Sci. & Tech.*, Kerman, pp. 571-578.

18. Hosseini, S. R., Ashrafizadeh, F. & Kermanpur, A. (2007). Calculation of compound layer thickness during nitriding process of pure iron, *Proc. 8th Conference Surface Engineering and Heat Treatment, Iranian Society of Surf. Sci. & Tech.*, Kerman, pp. 562-570.

19. Hosseini, S. R., Ashrafizadeh, F. & Kermanpur, A. (2009). Analytical-experimental approach for accurate depth profile evaluation of diffusion zone in plasma nitrided iron. *Surface Engineering*, DOI: 10.1179/174329409X439069.

20. Wriedt, H. A., Gokcen, N. A. & Nafziger, R. H. (1997). The Fe-N (Iron–Nitrogen) system. *Bull. of Alloy Phase Diagrams*, Vol. 8, pp. 355.

21. Sun, Y. & Bell, T. (1997). A numerical model of plasma nitriding of low alloy steels. *Mater. Sci. and Eng. A*, Vol. 224, pp. 33-47.

22. Sun, Y. & Bell, T. (1997). Computer prediction of threshold nitriding potential curves. *Heat Treatment of Metals*, Vol. 24, pp. 43-49.